IOPscience iopscience.iop.org

Home Search Collections Journals About Contact us My IOPscience

Optimizing single-photon-source heralding efficiency and detection efficiency metrology at 1550 nm using periodically poled lithium niobate

This article has been downloaded from IOPscience. Please scroll down to see the full text article.

2006 Metrologia 43 S56

(http://iopscience.iop.org/0026-1394/43/2/S12)

View the table of contents for this issue, or go to the journal homepage for more

Download details:
IP Address: 129.6.168.138
The article was downloaded on 20/01/2011 at 19:12

Please note that terms and conditions apply.

INSTITUTE OF PHYSICS PUBLISHING METROLOGIA
Metrologia **43** (2006) S56–S60 doi:10.1088/0026-1394/43/2/S12

Optimizing single-photon-source heralding efficiency and detection efficiency metrology at 1550 nm using periodically poled lithium niobate

S Castelletto[1], I P Degiovanni[1], V Schettini[1] and A Migdall[2]

[1] I.N.RI.M., Turin 10135, Italy
[2] NIST, Optical Technology Division, Gaithersburg, MD 20899-8441, USA

Received 26 October 2005
Published 23 March 2006
Online at stacks.iop.org/Met/43/S56

Abstract
We explore the feasibility of using high conversion-efficiency periodically-poled crystals to produce photon pairs for photon-counting detector calibrations at 1550 nm. The goal is the development of an appropriate parametric down-conversion (PDC) source at telecom wavelengths meeting the requirements of high-efficiency pair production and collection in single spectral and spatial modes (single-mode fibres). We propose a protocol to optimize the photon collection, noise levels and the uncertainty evaluation. This study ties together the results of our efforts to model the single-mode heralding efficiency of a two-photon PDC source and to estimate the heralding uncertainty of such a source.

1. Introduction

Parametric down-conversion (PDC) consumes pump photons and produces light with a two-photon field description [1]. This two-photon light, which allows one photon to indicate or herald the existence of its twin, has a key role in applications such as quantum radiometry [2], where it makes an independent primary standard method possible for direct photon-counting detector calibrations. In addition, this two-photon light is key for improving single-photon source schemes that have significant advantages over the attenuated laser sources often employed in quantum information applications [3, 4]. To realize a single-photon source [5] appropriate for these applications, we consider two key issues: (a) efficient photon pair production and (b) collection of the heralded photon in a single-mode fibre (SMF), which is of interest for telecom applications. Periodically poled crystals (PPLs) have been used for efficient pair production [6] but have not yet been used for metrology. While metrology applications would certainly benefit from the high pump-conversion efficiency of PPLs, characteristics such as the level of background fluorescence may limit the uncertainty that can be achieved.

As for the collection efficiency of PDC light into a SMF, the goal has been to understand how the detection of one photon of a PDC pair in a well-defined spatial and spectral mode defines its partner's spatial and spectral mode that can then be efficiently collected. Recent efforts have included experimental and theoretical work in both continuous wave (CW) [7–9] and pulse-pumped [10–12] bulk crystal PDC and have highlighted the critical problem of coupling the PDC photons into SMFs due to the difficulty of spatial and spectral matching of the photon pairs. The results show that optimization of the heralding efficiency is very sensitive to spectral and spatial mode selection.

Here we describe a PDC source and a measurement technique and compare them with other configurations. We present theoretical and experimental characterizations of the photon collection problem and suggest possible solutions.

2. Experimental setup

We pumped (figure 1) a 5 mm long periodically poled MgO-doped lithium niobate (PPLN) crystal with a CW laser at 532 nm. We used noncritical phase-matching (90° phase-matching angle) with a 7.36 µm poling period to produce 810 nm and 1550 nm photon pairs at external angles of 1° and 2°. We achieved fine tuning by adjusting the crystal temperature near 131 °C. Lens L_p in the pump beam produced

 © 2006 BIPM and IOP Publishing Ltd Printed in the UK

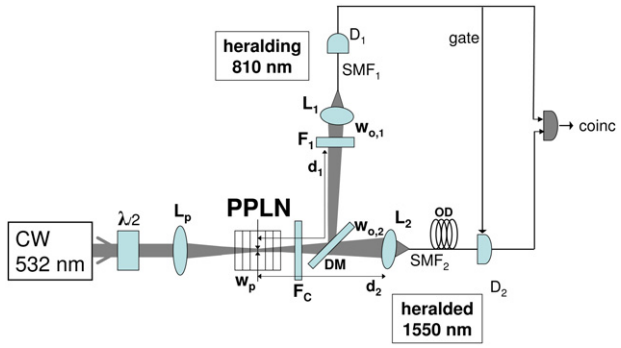


Figure 1. Setup to herald single photons from CW PDC in a PPLN crystal.
(This figure is in colour only in the electronic version)

Table 1. Measured and estimated Δ_1.

		Δ_1/nm	
d_1/mm	$w_{o,1}$/μm	measured	estimated
270	82	2.05	2.6
400	105	1.87	2.3
520	132	1.64	2.1

a Gaussian beam waist of $w_p \simeq 144\,\mu$m at the crystal; cutoff filter F_C blocked the pump laser and dichroic mirror DM separated the 810 nm (beam 1) and 1550 nm (beam 2) photons. An extra interference filter (F_1) at 810 nm with a full width at half-maximum (FWHM) of 10 nm suppressed extra fluorescence from the PPLN to reduce background heralding counts, while the SMF geometry imposed spectral selection with a heralding bandwidth, Δ_1 of ≈2 nm FWHM (see table 1). $L_{1,2}$ were aspheric coupling lenses of focal length 8 mm, AR-coated for 810 nm and 1550 nm. A monochromator in the heralding arm measured its spectral width. The heralding arm was routed to a SMF and then to D_1, a Si avalanche photodiode (APD), while the heralded arm also coupled to a SMF was sent to D_2, an InGaAs APD operating in gated mode. We gated the InGaAs detector with the detection of an 810 nm photon in the heralding arm and adjusted the delay in the heralded arm with appropriate length SMF and electronic cables. Calibrating the InGaAs detector, including the SMF and coupling lens optical losses against a conventional detector standard using an attenuated laser source, yielded a detection efficiency of $\eta_{\rm det} = 9.8\% \pm 0.5\%$ ($k = 1$, absolute uncertainty).

3. Measurement technique

The heralded D_2 detector efficiency as measured by the PDC source is given by

$$\eta_{\rm det} = \frac{\chi_{\rm D}}{\chi_{\rm P} \cdot \tau_{\rm opt} \cdot \tau_{\rm SMF-lens}}, \tag{1}$$

where $\chi_{\rm P}$ is the heralding efficiency (single-mode preparation efficiency, discussed in the next section) [8, 13], $\tau_{\rm opt}$ is the overall heralded arm optical transmittance (including PPLN, F_C and DM) and $\tau_{\rm SMF-lens}$ is the optical transmittance of L_2 and the SMF of the heralded arm. $\chi_{\rm D}$ is the raw D_2 channel detection efficiency, directly measured according to

$$\chi_{\rm D} = \frac{P_{\rm coinc} - P_{\rm uncorr}}{(1 - P_{\rm uncorr})(1 - P_{\rm backgnd}^{\rm heralding})}, \tag{2}$$

where $P_{\rm coinc}$ is the probability of coincidence counts per gate, $P_{\rm uncorr}$ is the probability of uncorrelated or accidental coincidence counts per gate (determined by changing the heralding delay so the detection gate misses heralded photons) and $P_{\rm backgnd}^{\rm heralding}$ is the probability of gating counts produced by uncorrelated photons and dark counts in the heralding arm.

3.1. Raw detection efficiency

To understand equation (2) we note that when D_1 fires, D_2 is gated for a duration T. We define the probability of D_2 not firing during T as p_T^0. We assume that the 'events' that make D_2 fire have a poissonian distribution (i.e. uniform in time). D_1 can fire for either background or PDC photons, and the associated probabilities are $P_{\rm backgnd}^{\rm heralding}$ and $P_{\rm PDC}^{\rm heralding} = 1 - P_{\rm backgnd}^{\rm heralding}$. The probability that D_2 fires for true correlated photons is $P_{\rm coinc}^{\rm heralded} = P_{\rm PDC}^{\rm heralding} p_{T/2}^0 \chi_{\rm D}$, where $p_{T/2}^0$ is the probability for the heralded detector to fire for the correlated photon arriving at $T/2$, as opposed to firing during the first half of the gating time. (We assume that correlated photons arrive exactly at $T/2$.) The probability that the heralded detector fires for accidental events is

$$P_{\rm acc} = (1 - p_T^0) P_{\rm backgnd}^{\rm heralding} + (1 - p_{T/2}^0) P_{\rm PDC}^{\rm heralding} + p_{T/2}^0 (1 - \chi_{\rm D})(1 - p_{T/2}^0) P_{\rm PDC}^{\rm heralding}. \tag{3}$$

The first term is the probability of an accidental coincidence due to D_1 firing for a background event and D_2 firing for any event. The second and third terms are for D_1 firing for a PDC event and D_2 firing due to a background event either before or after the arrival of the PDC photon at $T/2$. For D_2 to fire after $T/2$, it cannot have fired due to a background photon before $T/2$ or a PDC photon at $T/2$. These factors make up the third term. The total coincidence probability is $P_{\rm coinc} = P_{\rm coinc}^{\rm heralded} + P_{\rm acc}$. Considering that for poissonian statistics $p_T^0 = p_{T/2}^0 \times p_{T/2}^0$ and inverting the above equations, we obtain equation (2), where $P_{\rm uncorr} = 1 - p_T^0$.

3.2. Estimate and uncertainty

We develop an estimate of the raw detection efficiency and the associated uncertainty following [14]. The terms $P_{\rm coinc}$, $P_{\rm uncorr}$ and $P_{\rm backgnd}^{\rm heralding}$ in equation (2) are all independent statistical variables; therefore the estimate of the raw detection efficiency is

$$\langle \chi_{\rm D} \rangle = \left\langle \frac{1}{1 - P_{\rm backgnd}^{\rm heralding}} \right\rangle \times \left[1 - \left\langle \frac{1}{1 - P_{\rm uncorr}} \right\rangle (1 - \langle P_{\rm coinc} \rangle) \right]. \tag{4}$$

Applying the maximum likelihood (ML) model estimator to the random variables $P_{\rm coinc}$ and $P_{\rm uncorr}$, the probability of $M_{\rm coinc}$ coincidence counts given $M_{\rm heralding}$ heralding counts is

$$P(M_{\rm coinc} | M_{\rm heralding}, p) = \frac{M_{\rm heralding}!}{M_{\rm coinc}!(M_{\rm heralding} - M_{\rm coinc})!} \times p^{M_{\rm coinc}} (1 - p)^{M_{\rm heralding} - M_{\rm coinc}}, \tag{5}$$

where p is the parameter to estimate. The ML function is then

$$L(M_{\text{coinc}}, M_{\text{heralding}}|p) = P(M_{\text{coinc}}|M_{\text{heralding}}, p) \times P(M_{\text{heralding}}),$$

where $P(M_{\text{heralding}})$ is the distribution probability of heralding counts, which is not known. The minimum of the function $L(M_{\text{coinc}}|M_{\text{heralding}}, p)$ gives the estimate of P_{coinc}, without the need for $P(M_{\text{heralding}})$. It can be shown that $\langle P_{\text{coinc}}\rangle = \langle M_{\text{coinc}}/M_{\text{heralding}}\rangle$. The estimate of $\langle P_{\text{uncorr}}\rangle$ is less trivial. We must estimate $1/(1-P_{\text{uncorr}})$, as is clear from equation (4), so we introduce the parameter p' as $p = (p'-1)/p'$. The ML function in this case is

$$L(M_{\text{uncorr}}, M^{\text{delayed}}_{\text{heralding}}|p') = P(M_{\text{uncorr}}|M^{\text{delayed}}_{\text{heralding}}, p) \times P(M^{\text{delayed}}_{\text{heralding}}), \quad (6)$$

which we minimize to obtain

$$\langle(1/(1-P_{\text{uncorr}}))\rangle = \langle M^{\text{delayed}}_{\text{heralding}}/(M^{\text{delayed}}_{\text{heralding}} - M_{\text{uncorr}})\rangle.$$

We distinguished $M_{\text{heralding}}$ from $M^{\text{delayed}}_{\text{heralding}}$ because we measure heralding counts in two configurations, one in the presence of true coincidence photons and one without coincidences when an electronic delay line is added to the heralding arm. M_{uncorr} are the coincidences corresponding to uncorrelated events. For $P^{\text{heralding}}_{\text{backgnd}}$ the ML model is not applicable because we cannot measure it at the same time as the background counts M_{backgnd} and $M_{\text{heralding}}$, therefore we apply $\langle P^{\text{heralding}}_{\text{backgnd}}\rangle \approx \langle M_{\text{backgnd}}\rangle/\langle M_{\text{heralding}}\rangle$. This implies that $\langle P^{\text{heralding}}_{\text{backgnd}}\rangle$ must be close to 0, to have no impact on the estimate of the raw detection efficiency. We finally estimate

$$\langle\chi_{\text{D}}\rangle = \frac{1}{1-\langle M_{\text{backgnd}}\rangle/\langle M_{\text{heralding}}\rangle} \times \left[1 - \left\langle \frac{M^{\text{delayed}}_{\text{heralding}}}{M^{\text{delayed}}_{\text{heralding}} - M_{\text{uncorr}}}\right\rangle \times \left(1 - \left\langle \frac{M_{\text{coinc}}}{M_{\text{heralding}}}\right\rangle\right)\right], \quad (7)$$

with the uncertainty given by Gaussian uncertainty propagation for each random variable considered independently.

3.3. Heralding efficiency

The heralding efficiency χ_{P} is the efficiency of preparing a photon in the heralded channel in a definite spectral and spatial mode, by specific mode selection of the heralding arm. It quantifies how well the collection system geometrically catches photons correlated to those seen by D_1. To calibrate a SMF-coupled detector, the heralding efficiency must be optimized and estimated. It has been estimated in [8] for a bulk crystal. For PPLN [13] it is

$$\chi_{\text{P}} = \frac{4\, w_{\text{p}}^2 w_{\text{o},1}^2 w_{\text{o},2}^2 (w_{\text{o},1}^2 + w_{\text{p}}^2)}{(w_{\text{o},2}^2 w_{\text{p}}^2 + w_{\text{o},1}^2\,(w_{\text{o},2}^2 + w_{\text{p}}^2))^2} \times \frac{\Delta_2}{(\Delta_1^2 + \Delta_2^2)^{\frac{1}{2}}} \frac{f(c_1, c_2)}{f(s_1, s_2)}, \quad (8)$$

where $w_{\text{o},1,2}$ are the mode waists of the fibres at the crystal and $\Delta_{1,2}$ are the FWHM of the spectral distribution selected geometrically by the SMFs. f is a correction function accounting for crystal length (L) and PDC crystal frequency dispersion given by [12]

$$f(p,q) = \left\{ \int_0^1 \mathrm{d}x\, \mathrm{e}^{-px^2 + (q^2x^2/4p)} (\text{Erf}[qx/2\sqrt{p}] - \text{Erf}[(-2p+qx)/2\sqrt{p}]) \right\} \{\sqrt{p}\}^{-1}. \quad (9)$$

The parameters for this case are

$$c_1 = c_2 + \frac{L^2(w_{\text{p}}^2\alpha_{\text{s}}^2 + w_{\text{o},2}^2 \tan^2\theta_{\text{i}} + w_{\text{o},1}^2(\alpha_{\text{s}} + \tan\theta_{\text{i}})^2)}{w_{\text{o},2}^2 w_{\text{p}}^2 + w_{\text{o},1}^2(w_{\text{p}}^2 + w_{\text{o},2}^2)},$$

$$c_2 = \frac{L^2 D_{\text{is}}^2}{a^2} \frac{\Delta_1^2\Delta_2^2}{\Delta_1^2 + \Delta_2^2},$$

$$s_1 = \frac{L^2 D_{is}^2 \Delta_1^2}{a^2} + \frac{L^2(w_{\text{p}}^4\alpha_{\text{s}}^2 + w_{\text{o},1}^4(\alpha_{\text{s}} + \tan\theta_{\text{i}})^2)}{2w_{\text{o},1}^2 w_{\text{p}}^2(w_{\text{p}}^2 + w_{\text{o},1})} + \frac{L^2(2w_{\text{o},1}^2 w_{\text{p}}^2(\alpha_{\text{s}}^2 + \alpha_{\text{s}}\tan\theta_{\text{i}} + \tan^2\theta_{\text{i}}))}{2w_{\text{o},1}^2 w_{\text{p}}^2(w_{\text{p}}^2 + w_{\text{o},1}^2)},$$

$$s_2 = \frac{2L^2 D_{\text{is}}^2}{a^2} + \frac{L^2(w_{\text{p}}^2, \alpha_{\text{s}} + w_{\text{o},1}^2(\alpha_{\text{s}} + \tan\theta_{\text{i}})^2)}{w_{\text{o},1}^2 w_{\text{p}}^2(w_{\text{p}}^2 + w_{\text{o},1})}. \quad (10)$$

Here, $a = 2\sqrt{\ln(2)}$ converts between the FWHM and the Gaussian profile $1/\text{e}^2$ radius. The other terms are

$$D_{\text{is}} = D_{\text{i}}(\cos\theta_{\text{i}} - \sin\theta_{\text{i}}\tan\theta_{\text{i}}) - D_{\text{s}}(\cos\theta_{\text{s}} + \sin\theta_{\text{s}}\tan\theta_{\text{s}}),$$

$$D_{\text{pi}} = -D_{\text{i}}(\cos\theta_{\text{i}} + \sin\theta_{\text{i}}\tan\theta_{\text{i}}) + D_{\text{p}},$$

with

$$D_{\text{i,s}} = (\mathrm{d}n_{\text{i,s}}(\omega_{\text{i}}, \phi_{\text{o}})\omega_{\text{i,s}}/c)/(\mathrm{d}\omega_{\text{i,s}})|_{\Omega_{\text{i,s}}},$$

$$D_{\text{p}} = (\mathrm{d}n_{\text{p}}(\omega_{\text{p}}, \phi_{\text{o}})\omega_{\text{p}}/c)/(\mathrm{d}\omega_{\text{p}})|_{\Omega_{\text{p}}}.$$

$\alpha_{\text{s}} = -\cos\theta_{\text{s}}\tan\theta_{\text{i}} + \sin\theta_{\text{s}}$. $\theta_{\text{i,s}}$ are the associated idler and signal emission angles around $\phi_{\text{o}} = \pi/2$ (the phase-matching angle in a non-critical phase-matching configuration) and $n_{\text{i,s,p}}(\omega_{\text{i,s,p}}, \phi_{\text{o}})$ are the indices of refraction (all are e-rays) at the three frequencies. $\Omega_{\text{i,s,p}}$ are the central angular frequencies.

For our experiment the fibre mode field diameters are $\text{MFD}_1 = 3.9\,\mu\text{m}$ for the heralding arm and $\text{MFD}_2 = 5.6\,\mu\text{m}$ for the heralded arm, giving mode waists $w_{\text{o},1,2} = M_{1,2}\,\text{MFD}_{1,2}$ at the crystal according to the magnification ($M_{1,2}$) used. Because of this, we identify a SMF as a spectral filter with a gaussian spectral distribution given by $\widetilde{I}_{\text{s,i}}(\omega_{\text{s,i}} - \Omega_{\text{s,i}}) \propto \mathrm{e}^{-(a^2/\Delta_{1,2}^2)(\omega_{\text{s,i}} - \Omega_{\text{s,i}})^2}$. The component of spectral width due to geometric selection, $\Delta_{1,2}$, is given by the FWHM angular collection $\Delta\theta_{1,2} = a(\lambda_{\text{i,s}})/(\pi w_{\text{o},1,2})$ and the spectral/angular spread of the PDC, $\theta_{\text{i,s}}(\lambda_{\text{s,i}})$ around the central wavelength $\lambda_{\text{i,s}}$. Here, because the non-degenerate PPLN configuration and the bandwidth estimation are critical, we measured it with a monochromator in the heralding arm. We spectrally scanned the heralding single counts at three different values of $w_{\text{o},1}$ (table 1). We also theoretically estimated these bandwidths by evaluating the FWHM of the phase-matching function according to [15], extended to the case of PPLN. Here we consider the PDC phase-matching function including the pump transverse distribution

$$\Phi(\omega_{\text{s}}, \theta_{\text{i}}, \theta_{\text{s}}) = \exp\left(-\frac{w_{\text{p}}^2(\Delta k_x^2 + \Delta k_y^2)}{4}\right) \times \left(\frac{\sin\Delta k_z L}{\Delta k_z L}\right)^2. \quad (11)$$

$\Delta k_{x,y,z}(\omega_s, \theta_i, \theta_s)$ are the mismatch of the k-wavevectors $\Delta k_{x,y,z} = (\boldsymbol{k}_p - \boldsymbol{k}_s - \boldsymbol{k}_i)_{x,y,z}$, in terms of the pump, signal and idler k-vectors:

$$\Delta k_z = \frac{n(\omega_p)\omega_p}{c} - \frac{n(\omega_s)\omega_s}{c}\cos\theta_s - \frac{n(\omega_i)\omega_i}{c}\cos\theta_i - \frac{2\pi}{\Lambda},$$

$$\Delta k_{x,y} = \frac{n(\omega_s)\omega_s}{c}\sin\theta_s + \frac{n(\omega_i)\omega_i}{c}\sin\theta_i,$$

where Λ is the poling period. To estimate the bandwidth selected by the heralding arm fibre, we first find θ_i^{max} that maximizes equation (11) and then we consider for each wavelength the function $f(\theta_s, \omega_s) = 1$ for $\Phi(\omega_s, \theta_i^{max}, \theta_s) > 0.5$ and $f(\theta_s, \omega_s) = 0$ for $\Phi(\omega_s, \theta_i^{max}, \theta_s) < 0.5$. Finally we invert the functions $f(\theta_s + \Delta\theta_1/2, \omega_s)$ and $f(\theta_s - \Delta\theta_1/2, \omega_s)$ to determine Δ_1.

We estimated the heralded arm bandwidth in the same way. This estimation, which was found to be in agreement with the experimental values, allowed us to extrapolate the bandwidths of the heralded arm for other configurations. The discrepancy between the estimated and measured values is likely due to using Sellmeier's equations [16] for undoped PPLN. Moreover, we do not have precise knowledge of the crystal poling region length (it maybe slightly shorter than the full 5 mm crystal length), a crucial engineering parameter. In figure 2 we report the estimated χ_p versus $w_{o,1,2}$ for our experiment's fixed pump waist, and crystal length in two spectral-selection configurations on the heralding arm: (*a*) the SMF acts as a spectral filter with an average FWHM of about 2 nm and (*b*) a FWHM 0.1 nm spectral filter (a monochromator was used for this narrow bandwidth). The two experimental conditions for the measurements in table 2 are roughly indicated in figure 2(*a*) by squares, while the conditions for the narrow band measurement are indicated in figure 2(*b*). While the heralded arm is spectrally selected only by the fibre, the large improvement achieved by narrowing the heralding bandwidth indicates that spectral mode matching is more critical than spatial mode matching (the only spatial requirement is that $w_{o,2} \cong w_p$, $w_{o,1} > w_p$). Using this we should be able to improve χ_p by further narrowing the heralding arm bandwidth.

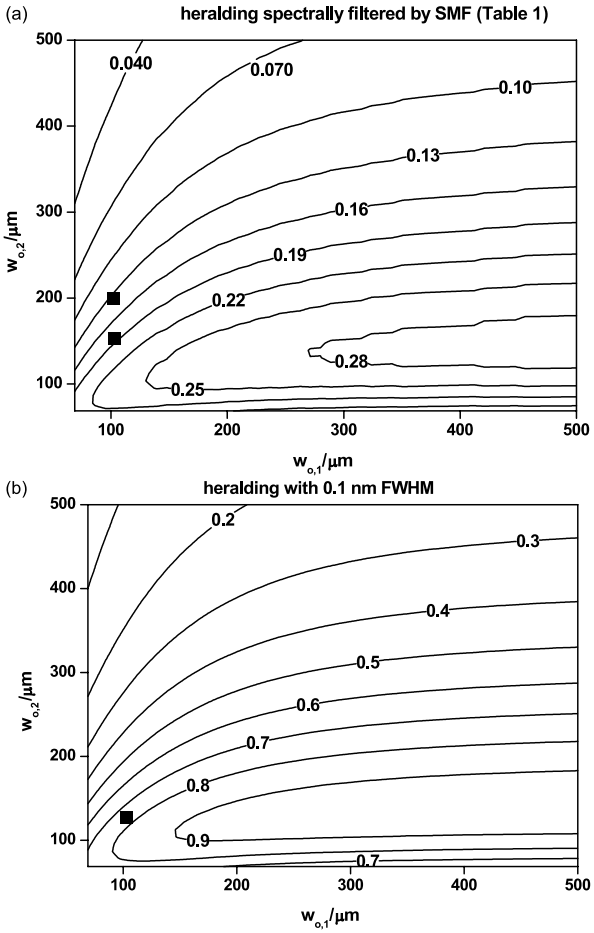


Figure 2. Calculated χ_p versus heralding and heralded waists (*a*) without an interference filter and (*b*) with spectral filtering on the heralding arm of 0.1 nm FWHM. Estimated values in the experimental conditions are given by the black squares. $w_p = 144\,\mu m$ in both parts.

Table 2. Measured χ_D with the estimate, ML uncertainty and statistical fluctuations.

$w_{o,2} = 158\,\mu m$			$w_{o,2} = 197\,\mu m$		
χ_D	σ_{ML}	σ_{stat}	χ_D	σ_{ML}	σ_{stat}
2.508%	0.044%	0.040%	2.015%	0.030%	0.028%
2.555%	0.025%	0.019%	2.056%	0.028%	0.035%
2.584%	0.036%	0.031%	2.107%	0.034%	0.028%
2.489%	0.039%	0.037%	1.996%	0.032%	0.026%

4. Experimental results

Following the approach in section 3.2, we measured the raw detection efficiency in our setup at the best signal-to-noise ratio of the heralding arm. Table 2 shows χ_D measured with $w_{o,1} = 82\,\mu m$ fixed ($d_1 = 270$ mm) for two different positions of the heralded arm, corresponding to $w_{o,2} = 158(197)\,\mu m$ ($d_2 = 300(380)$ mm). The estimates and uncertainties calculated with this model and the measured intrinsic statistical fluctuations show good agreement. For each setup we tested the repeatability by applying our alignment procedure [2] over several days. Figure 3 shows the measurement repeatability in agreement with the estimated uncertainty at the $2\sigma_{ML}$ level. However, we point out that the repeatability test was limited to collection lens positions close to the source. We obtained theoretical values of $\chi_p = 20\%$ and 13%, respectively, for the waists in table 2 using only the SMF spectral selectivity. The decrease in χ_p for bigger $w_{o,2}$ is in agreement with the measured decrease in χ_D. Our theoretical model for χ_p is very sensitive to the measurements of the beam waists and the bandwidth estimates. Estimating the optical transmittances at $\tau_{opt} = 65\%$ and $\tau_{SMF-lens} = 83\%$ by an independent calibration and using the measured χ_D in table 2, we were able to consistently obtain $\chi_p = 48\%$, 37%. On occasion we measured χ_p much closer to one by inserting a monochromator in the heralding arm; however, the stability of our setup did not allow repeatable results at this level.

At this stage, we note that the model can only be considered qualitative due to the spectral approximation adopted. In our approach we limited the calculation of the mismatch term to first order in the transverse k-vector and the frequency, losing some of the correlation between the frequency and the spatial variables in the biphoton field [12]. To compensate, we introduced a selection term due to the SMF spatial selection, but this works best for the degenerate

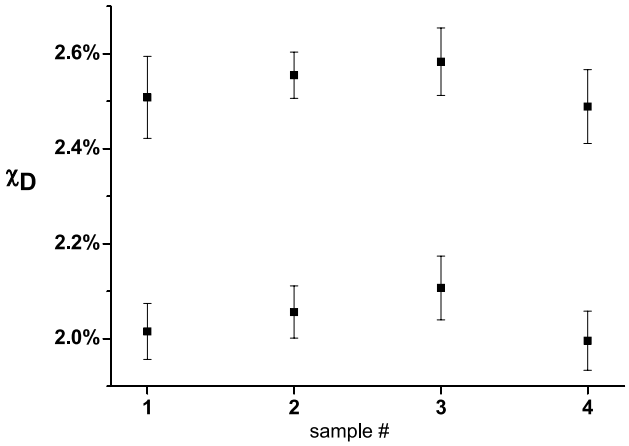


Figure 3. Repeated measurements of χ_D for two setups ($k = 2$ ML uncertainty shown).

case where the PDC emission is broader and this correction has less of an effect on the final mode matching than in the nondegenerate case. This case requires a full numerical solution.

5. Conclusions

We have shown the feasibility of using PPLN for single-photon detector calibration at 1550 nm, as well as for a single-photon single-mode source. We highlighted the need to maintain low dark counts in the heralding arm to reduce statistical fluctuations. We have shown that proper spatial mode matching and spectral mode selection in the heralding arm is of paramount importance in achieving the highest heralding efficiency.

Acknowledgment

This work was supported in part by DTO, ARO and DARPA/QUIST.

References

[1] Klyshko D N 1988 *Photons and Nonlinear Optics* (London: Gordon and Breach)
[2] Migdall A L, Castelletto S, Degiovanni I P and Rastello M L 2002 *Appl. Opt.* **41** 2914–22
[3] Tittel W, Brendel J, Zbinden H and Gisin N 2000 *Phys. Rev. Lett.* **84** 4737–40
[4] Knill E, Laflamme R and Milburn G J 2001 *Nature* **409** 46–52
[5] Fasel S, Alibart O, Tanzilli S, Baldi P, Beveratos A, Gisin N and Zbinden H 2004 *New J. Phys.* **6** 163
[6] Albota M A and Dauler E 2004 *J. Mod. Opt.* **51** 1417–32
[7] Kurtsiefer C, Oberparlieter M and Weinfurter H 2001 *Phys. Rev.* A **64** 023802
[8] Castelletto S, Degiovanni I P, Migdall A, Schettini V and Ware M 2004 *Proc. SPIE* **5551** 60–72
[9] Ljunggren D and Tengner M 2005 *Preprint* quant-ph/0507046
[10] Bovino F A, Varisco P, Colla A M, Castagnoli G, Di Giuseppe G and Sergienko A V 2003 *Opt. Commun.* **227** 343–8
[11] Pittmann T B, Jacobs B C and Franson J D 2005 *Opt. Commun.* **246** 545–50
[12] Castelletto S, Degiovanni I P, Schettini V and Migdall A 2005 *Opt. Express* **13** 6709–22
[13] Castelletto S, Degiovanni I P, Schettini V and Migdall A 2005 *Proc. SPIE* **5893** 288–99
[14] Castelletto S, Degiovanni I P and Rastello M L 2002 *J. Opt. Soc. Am.* B **19** 1247–58
[15] Boeuf N, Branning D, Chaperot I, Dauler E, Guerin S, Jaeger G, Muller A, Migdall A 2000 *Opt. Eng.* **39** 1016–24
[16] Jundt D H 1997 *Opt. Lett.* **22** 1553–5